Available online at www.sciencedirect.com

ScienceDirect

Geochimica et Cosmochimica Acta 134 (2014) 120–136

Geochimica et Cosmochimica Acta

www.elsevier.com/locate/gca

Evaluation of kinetic effects on clumped isotope fractionation (Δ_{47}) during inorganic calcite precipitation

Jianwu Tang [a,*], Martin Dietzel [b], Alvaro Fernandez [a], Aradhna K. Tripati [c,d], Brad E. Rosenheim [a,1]

[a] Department of Earth & Environmental Sciences, Tulane University, New Orleans, LA 70118-5698, USA
[b] Institute of Applied Geosciences, Graz University of Technology, Rechbauerstrasse 12, 8010 Graz, Austria
[c] Department of Earth and Space Sciences, Institute of Geophysics and Planetary Physics, University of California, Los Angeles, CA 90095, USA
[d] Department of Atmospheric and Oceanic Sciences, Institute of the Environment and Sustainability, University of California, Los Angeles, CA 90095, USA

Received 17 September 2013; accepted in revised form 4 March 2014; available online 24 March 2014

Abstract

Considerable efforts have been made to calibrate the Δ_{47} paleothermometer, which derives from the quantity of ^{13}C–^{18}O bonds in carbon dioxide produced during acid digestion of carbonate minerals versus its expected stochastic abundance, in a range of materials. However the impacts of precipitation rate, ionic strength, and pH on carbonate Δ_{47} values are still unclear. Here we present a set of 75 measurements of Δ_{47} values from inorganic calcites grown under well-controlled experimental conditions, where we evaluate the impact on Δ_{47} values of precipitation rate ($\log R = 1.8$–4.4 μmol/m^2/h), pH (8.3–10.5; NBS pH scale), and ionic strength ($I = 35$–832 mM). With the data available and at the current instrumental resolution, our study does not resolve any clear effects of pH, ionic strength, growth rate effects on measured Δ_{47} when compared in magnitude to the effects on $\delta^{18}O$ over most of the ranges of parameters sampled by our analyses. If these relationships exist, they must be smaller than our current ability to resolve them within our dataset. Under our experimental conditions, a Δ_{47}-temperature equation, which is apparently insensitive to variation in pH, precipitation rate, and ionic strength over the range of variables sampled, can be written as

$$\Delta_{47} = (0.0387 \pm 0.0072) \times 10^6/T^2 + (0.2532 \pm 0.0829) \quad (r^2 = 0.9998,\ p = 0.009)$$

where Δ_{47} values were reported on the absolute Δ_{47} reference frame after normalizing to conventional 25 °C reaction temperature using an acid fractionation factor of $-0.00141‰$ °C^{-1}.
© 2014 Elsevier Ltd. All rights reserved.

1. INTRODUCTION

The stable oxygen isotopic fractionation between carbonates and water can be used to estimate paleo-temperature (Urey, 1947; Epstein et al., 1951, 1953). Use of this traditional oxygen isotope thermometer is dependent on knowledge of the oxygen isotope composition ($\delta^{18}O_{water}$) of the water from which the carbonate mineral precipitated. However, for most geological materials, we can only measure $\delta^{18}O$ of the carbonate mineral ($\delta^{18}O_{carbonate}$) without constraint on the two main variables that influence $\delta^{18}O_{carbonate}$ (temperature and $\delta^{18}O_{water}$). Most work on carbonates relies on independent paleothermometers such as carbonate Sr/Ca and Mg/Ca ratios to interpret changes in $\delta^{18}O_{water}$ (Flower and Kennett, 1990; Spero and

* Corresponding author.
E-mail address: jianwu.tang@gmail.com (J. Tang).
[1] Present address: College of Marine Science, University of South Florida, St. Petersburg, FL 33701, USA.

http://dx.doi.org/10.1016/j.gca.2014.03.005
0016-7037/© 2014 Elsevier Ltd. All rights reserved.

Williams, 1990; Hendy et al., 2002; Flower et al., 2004; Schmidt et al., 2004; Rosenheim et al., 2005; Lund and Curry, 2006; Moses et al., 2006; Schmidt et al., 2006; Schmidt and Lynch-Stieglitz, 2011) or assumptions about the isotopic composition of the waters of formation (e.g., Rosenheim et al., 2009). Despite the high precision of elemental ratio measurements, the propagation of uncertainties from empirical calibration to temperature into $\delta^{18}O_{water}$ values can be significant (e.g., Schmidt, 1999; Rosenheim et al., 2005). In addition, on long enough time scales, changes in the cationic composition of seawater also need to be considered when interpreting elemental proxies.

In contrast to stable oxygen isotope composition, the carbonate clumped isotope thermometer is independent of the isotopic composition of water from which the carbonate mineral precipitates (Ghosh et al., 2006). This paleothermometer is based on the temperature dependence of ^{13}C–^{18}O bond abundance in the carbonate crystal lattice. The clumping of ^{13}C and ^{18}O into bonds with each other in the crystal lattice involves a homogeneous isotope exchange reaction within one single mineral phase (Schauble et al., 2006). Therefore, the advantage of the carbonate clumped isotope thermometer is the potential to more directly estimate the precipitation temperature of carbonates using the measurement of ^{13}C–^{18}O bond abundance in carbonates. Subsequently, the $\delta^{18}O_{water}$ can be calculated using simultaneous measurements of $\delta^{18}O_{carbonate}$.

Early studies (Ghosh et al., 2006) linked the abundance of ^{13}C–^{18}O bonds in CO_2 liberated by phosphoric acid digestion of a carbonate mineral to that in the reactant carbonate mineral. The isotopic species $^{13}C^{18}O^{16}O$ accounts for most of the mass 47 CO_2 measured by isotope ratio mass spectrometry. The abundance of this species is reported using the notation Δ_{47}, representing the mass 47 enrichment in CO_2 relative to the amount of mass 47 expected for a CO_2 that has the same bulk isotopic composition but a stochastic distribution of isotopologues (Wang et al., 2004). Specifically Δ_{47} is defined as:

$$\Delta_{47} = \left[\frac{R^{47}}{2R^{13}\cdot R^{18} + 2R^{17}\cdot R^{18} + R^{13}\cdot (R^{17})^2} - \frac{R^{46}}{2R^{18} + 2R^{13}\cdot R^{17} + (R^{17})^2} - \frac{R^{45}}{R^{13} + 2R^{17}} + 1 \right] \cdot 1000$$

where R refers to the ratio of the minor isotopologue to the major isotopologue of the molecule of interest.

In 2006, Ghosh et al. published the first Δ_{47}-temperature calibration that was based on inorganic calcite precipitation at controlled temperatures using a classical active degassing method (i.e., CO_2 was removed from a solution containing Ca^{2+} and HCO_3^- and purged by N_2 gas), as well as biogenic, aragonitic deep-sea and tropical corals. Following this pioneering work, further investigations of the relationship between Δ_{47} and calcifying temperature were carried out using different biogenic carbonates (Came et al., 2007; Ghosh et al., 2007; Eagle et al., 2010, 2013; Tripati et al., 2010; Thiagarajan et al., 2011; Zaarur et al., 2011; Saenger et al., 2012; Dennis et al., 2013; Grauel et al., 2013; Henkes et al., 2013), inorganic synthetic carbonates (Dennis and Schrag, 2010; Zaarur et al., 2013), and theoretical calculations (Schauble et al., 2006; Guo et al., 2009; Hill et al., 2013). All calibration datasets show evidence of correlation between Δ_{47} and temperature, although there are some discrepancies among the calibrations (Fig. 1, see also Fernandez et al., 2014 for analysis of these calibrations). Many biogenic carbonates (Ghosh et al., 2006, 2007; Came et al., 2007; Eagle et al., 2010; Tripati et al., 2010; Thiagarajan et al., 2011; Grauel et al., 2013) exhibit a Δ_{47} sensitivity to temperature that is similar to the original inorganic calibration of Ghosh et al. (2006), if the Ghosh et al. (2006) data are transferred onto the absolute reference frame (Dennis et al., 2011). The Ghosh et al. (2006) calibration is generally used as the nominal equilibrium calibration due to the fact that it succeeds in explaining the Δ_{47} of most biogenic carbonates surveyed thus far. Recently, the Ghosh et al. (2006) calibration was re-examined by Zaarur et al. (2013) who conducted additional carbonate precipitation experiments and ran their samples at higher analytical precision directly applying an absolute reference frame (Dennis

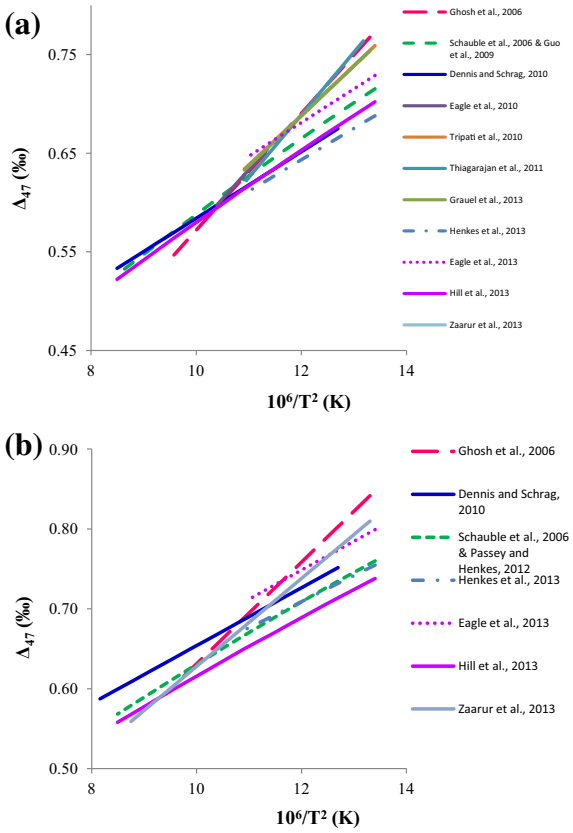

Fig. 1. Published Δ_{47}-temperature calibration lines from biogenic carbonates and inorganic synthetic calcites: (a) Δ_{47} data are reported on the heated gas reference frame (Huntington et al., 2009); (b) Δ_{47} data are reported on the absolute reference frame (Dennis et al., 2011). Hill et al. (2013) theoretical calculations for calcite are shown with an acid digestion fractionation factor of 0.232‰ in the heated gas reference frame and an acid digestion fractionation factor of 0.268‰ (from Passey and Henkes, 2012) in the absolute reference frame. To facilitate comparison with other studies, Henkes et al. (2013) data were corrected with an acid digestion fractionation factor of 0.08‰ for the 90–25 °C offset from Passey et al. (2010).

et al., 2011). The revised calibration by Zaarur et al. (2013) has a similar slope as the original calibration, which further confirms that the Ghosh et al. (2006) calibration can be considered as the nominal equilibrium calibration.

Deviations of Δ_{47} from values predicted by the Ghosh et al. (2006) calibration are generally discussed in terms of non-equilibrium clumped isotopic fractionation (Affek et al., 2008; Daëron et al., 2011; Kluge and Affek, 2012; Dennis et al., 2013). For example, such deviations have been proposed as a new tool to quantify kinetic fractionation in modern speleothems (Kluge and Affek, 2012). More recently, however, a few biogenic carbonates (Zaarur et al., 2011; Dennis et al., 2013; Eagle et al., 2013; Henkes et al., 2013) exhibit lower Δ_{47} sensitivity to temperature that is more similar to the calibration published by Dennis and Schrag (2010).

The reasons for the discrepancies in temperature sensitivity between four inorganic synthetic calcite calibration lines, and different populations of biogenic data, are still unclear. These differences may reflect a combination of factors including the nature of the samples used for calibration, kinetic effects associated with sample growth, uncertainties in growth temperatures for field-collected materials, analytical artifacts, and/or standardization. The latter explanation has been explored by Dennis et al. (2011), who proposed that the use of an absolute reference frame to standardize data between laboratories should minimize potential measurement artifacts. Even after translating clumped isotope data of Ghosh et al. (2006) and of Dennis and Schrag (2010) into the absolute reference frame (Dennis et al., 2011), the discrepancy between inorganic calibrations still remains (Fig. 1b).

Theoretical predictions of the slope relating temperature of precipitation to Δ_{47} are similarly uncertain (Fig. 1). Initial theoretical calculations for calcite based on first-principles modeling (Schauble et al., 2006; Guo et al., 2009) indicate lower Δ_{47} temperature sensitivity (shallower slope) similar to that of Dennis and Schrag (2010), although uncertainties in the calculations are reasonably large. In addition, subsequent work has shown that anharmonic corrections to theoretical calculations can be significant (Cao and Liu, 2012) and these were not considered in earlier studies. Other recent work has shown that the choice of model and basis set used for theoretical calculations has a significant effect on predictions of clumped isotope fractionations (Hill et al., 2013).

Experimental conditions (pH, precipitation rate) in previous calibration studies (Ghosh et al., 2006; Dennis and Schrag, 2010; Zaarur et al., 2013) were not truly constrained (e.g., pH and also precipitation rate varied through the experiment), and therefore it is feasible neither to evaluate whether kinetic effects arising from experimental conditions may have dominated one or all of those calibration lines (Ghosh et al., 2006; Dennis and Schrag, 2010; Zaarur et al., 2013), nor to determine which of these inorganic calcite calibration lines approaches isotopic equilibrium. Recent theoretical studies (Tripati et al., in revision; Hill et al., 2013) suggest that pH and salinity can, in principle, have a weak effect on Δ_{47} values in carbonate minerals if growth rates are sufficiently rapid (e.g., immediate precipitation of $BaCO_3$ by mixing the $NaHCO_3$ solution with $BaCl_2$ and NaOH solution).

Here, to evaluate the potential scope of kinetic isotope effects associated with growth rate, pH, and ionic strength on clumped isotope signatures in inorganic calcite, we measured synthetic samples in two laboratories. To briefly summarize, this paper reports a set of 75 Δ_{47} values measured from inorganic calcite grown in laboratory experiments using an advanced CO_2 diffusion technique (Dietzel and Usdowski, 1996; Dietzel et al., 2004; Tang et al., 2008). This technique was used because it is relatively easy to (1) control physicochemical conditions of calcite precipitation, (2) precisely determine the precipitation time and $CaCO_3$ precipitation rate, and (3) calculate the saturation index when calcite starts to precipitate. Calcite was precipitated at three different temperatures (5, 25, and 40 °C), a wide range of pH ($8.3 \leqslant pH \leqslant 10.5$) and precipitation rates ($1.8 \leqslant \log R \leqslant 4.4$ μmol/m^2/h), and at three ionic strengths (35, 292, and 832 mM), allowing evaluation of the potential impact of those parameters on Δ_{47}. In some experiments, DIC has reached equilibrium with water prior to calcite precipitation. In other experiments, it has not reached equilibrium.

2. METHODS

2.1. Inorganic calcite precipitation

Inorganic calcite was precipitated from homogeneous solutions using an advanced CO_2-diffusion technique adapted from Dietzel and Usdowski (1996) and Dietzel et al. (2004). Experimental set-up, mineral and chemical analysis, and calculations of precipitation rate are described in detail elsewhere (Tang et al., 2008). In brief, a 0.5 L solution of 0.83 M $NaHCO_3$ was separated from a 5 L solution of 0.01 M $CaCl_2$ by a polyethylene (PE) membrane. In order to buffer the pH, 1.34 g of NH_4Cl (to make a 5 mM NH_4Cl solution) was added to the $CaCl_2$ solution. According to Dietzel et al. (2004), the PE membrane allows CO_2 diffusion from the $NaHCO_3$ solution to $CaCl_2$ solution, but prevents any kind of ionic diffusion such as Ca^{2+} diffusion from the$CaCl_2$ solution to the $NaHCO_3$ solution. Compared to the $CaCl_2$ solution, the $NaHCO_3$ solution has a significantly higher internal P_{CO_2} and thus CO_2 diffuses at an almost constant rate from the $NaHCO_3$ solution through the PE membrane into the $CaCl_2$ solution. With increasing dissolved inorganic carbon (DIC) concentrations in the $CaCl_2$ solution, calcite precipitates at a distinct saturation index threshold. During all experiments, the $CaCl_2$ solution was stirred by a regular magnetic stirring bar at 300 rpm or a floating stirring bar (Nalgene® Labware, DS6630-4000) at 200 rpm so that calcite crystals were growing from a well-agitated homogeneous solution. The pH of the $CaCl_2$ solution was kept constant by pH-stat titration of a 2 M NaOH solution with an accuracy of ±0.03 (Schott TitroLine alpha plus). The pH of the solution was measured by a pH combination electrode (Schott Blue Line 28 pH Pt 1000), calibrated at 25 °C with NIST certified buffer solutions (pH 4.01, 7.00, and 10.00). By using this pH-stat titration technique, calcite precipitation at a constant

pH is guaranteed. From the titration curve for each experiment (Tang et al., 2008), the time point for the first precipitation as well as DIC concentration at that time can be estimated. This allows us to calculate the precipitation rate and the apparent saturation index (Tang et al., 2008). The precipitation rate for each experiment can be adjusted by the thickness of (PE) membrane as well as the pH of the $NaHCO_3$ solution. Because precipitation rate is essentially controlled by the CO_2 uptake rate in the $CaCl_2$ solution, an almost constant CO_2 uptake rate lets calcite grow at nearly constant precipitation rate, verified by the titration curve of each experiment (Tang et al., 2008).

Experiments were conducted at three different temperatures (5, 25, and 40 °C). For experiments at 5 and 40 °C, the whole experimental set-up was installed in a temperature-controlled chamber (VötschIndustrietechnik VC 4033) with a temperature variation of less than ±0.5 °C. Experiments at 25 °C were conducted in the above temperature-controlled chamber, in a temperature regulated laboratory, or in a water bath with a temperature variation of less than ±0.5 °C. For experiments at 5 and 40 °C, all calcite was grown from $CaCl_2$ solutions with an ionic strength of 35 mM. For experiments at 25 °C, three ionic strengths (35, 292, and 832 mM) were used for the $CaCl_2$ solution to investigate the effects of changing ionic strength (Tang et al., 2012); for reference the ionic strength of seawater is in the vicinity of 700 mM. This is achieved by adding 257 or 797 mM NaCl into the initial 35 mM $CaCl_2$ solution. All aqueous solutions were prepared using deionized water (18.2 MΩ cm, Elga Purelab Maxima) and reagent grade chemicals ($CaCl_2{\cdot}2H_2O$, $SrCl_2{\cdot}6H_2O$, NH_4Cl_4; NaCl, NaOH, $NaHCO_3$, and NH_4Cl, Merck p.a.).

At the end of each experiment, suspended calcite crystals were collected by filtering the $CaCl_2$ solution through a 0.2 μm cellulose acetate membrane. Crystals adhering to container walls were removed using a plastic wiper. Crystals were rinsed with deionized water and dried at 40 °C in an oven. The presence of a calcite mineral phase was verified by X-ray diffraction (goniometer type Philips PW 1130/1370), infrared spectroscopy (Perkin Elmer 1600), and micro Raman spectroscopy (Labram HR-800UV). Inspection of samples using scanning electron microscopy (Zeiss Ultra 55, see Tang et al., 2008) revealed that crystals had the typical rhombohedral habit of calcite.

The precipitation rate of calcite sample from each experiment was calculated from the total amount of calcite precipitated, the precipitation time, and the specific surface area of calcite as described elsewhere (Tang et al., 2008). The amount of precipitated calcite was obtained by monitoring the decrease in Ca^{2+} concentrations in the $CaCl_2$ solutions. Precipitation time was determined from the titration curve. The specific surface area for calcite of each experiment was estimated from particle size distribution analyses of the final solid phase using a centrifugal particle size analyzer (Shimadzu SA-CP2; see Tang et al., 2008 for more details).

2.2. Clumped isotope measurements

Clumped isotope measurements were performed in two laboratories. The majority of analyses were done at Tulane University using an Isoprime dual inlet isotope ratio mass spectrometer modified to simultaneously measure masses 44–49 as described in Rosenheim et al. (2013). Replicate measurements of the 5 °C experiments were made in the Tripati Lab at University of California, Los Angeles (UCLA, using a specially modified Thermo Fisher 253 gas source mass spectrometer dedicated to measuring clumped isotopes in CO_2). Sample preparation at Tulane was different than at UCLA.

2.2.1. Sample digestion, purification, and measurement

At Tulane, about 25 mg of carbonate was digested under vacuum in concentrated phosphoric acid ($\rho = 1.93$ g/ml). All digestion reactions were conducted at 100 °C using a boiling water bath, except one that was done at 25 °C using a temperature-controlled water bath. The reaction time for 100 °C digestion was about 20 min or less, depending on carbonate crystal size, and reaction time for 25 °C digestion was more than 12 h. During calcite digestion at 100 °C, CO_2 was actively removed by a liquid N_2 trap. Then, CO_2 was expanded into a glass vacuum line through warming of the frozen CO_2 from −195 to −70 °C by replacing the liquid N_2 trap with a frozen isopropyl alcohol water trap. Subsequently, CO_2 was purified using a U-shaped PoraPak Q trap held at −15 °C using frozen ethylene glycol. After passing through the PoraPak Q trap twice, CO_2 was frozen into a small evacuated container and transferred to the inlet of the mass spectrometer.

At UCLA, sample and standards are processed using a custom-built automated system for digestion and purification (after Passey et al., 2010), which is attached to a gas-source mass spectrometer that has been configured for the analysis of multiply substituted isotopologues of CO_2. The carbonate sample digestion system is composed of (1) a Costech Zero Blank autosampler made of stainless steel that will pull high vacuum, (2) a common acid bath for phosphoric acid digestion of samples, (3) cryogenic traps (dry ice and ethanol, and liquid nitrogen) for the purification and collection of CO_2 and removal of water and other gases with low vapor pressures, (4) a gas chromatograph with a packed column and a cryogenic trap to further purify CO_2 through the removal of organic contaminants, with helium being used as a carrier gas, (5) cryogenic traps to separate prepared gases from the helium, (6) a final set of valves and traps to purify CO_2 and transfer it into the bellows of the mass spectrometer. In this system, at least 8 mg of calcite powder are digested at 90 °C in phosphoric acid ($\rho = 1.92$ g/ml) in order to ensure a sufficient amount of CO_2 for stable voltages over the course of several hours of mass spectrometric analysis. The reaction time was 20 min in a common acid bath system, with acid changed after every 10–15 analyses. The resultant gas was actively removed into a metal trap immersed in liquid N_2, passing through a glass water trap immersed in a dewar of ethanol at −70 °C. After two rounds of cryogenic purification to remove water, CO_2 was then passed through a gas chromatograph containing a column filled with PoraPak Q that is at −20 °C, and then recleaned cryogenically as described above to remove any additional water before being transferred to the inlet of the mass spectrometer. Measurements

are made to yield a stable 16-volt signal for mass 44, with peak centering, pressure baseline measurement (He et al., 2012), and pressure balancing before each acquisition.

2.2.2. Standardization and reproducibility of measurements

In order to report our measured Δ_{47} values on a common scale (Dennis et al., 2011), at SILT U we first constrained our instrument's reference frame by analyzing a set of heated gases and three sets of low-temperature equilibrated gases (4.5, 28, and 51 °C). Heated gases were prepared by sealing a set of CO_2 gases (whose δ47 range between −55‰ and 20‰ relative to the reference gas) into quartz ampoules and heating at 1000 °C for at least 2 h in a muffle furnace. Low-temperature equilibrated gases were prepared by equilibrating CO_2 with approximately 150 μL of water of different isotope composition in sealed borosilicate ampoules for 24–96 h at 4.5, 28, and 51 °C. Details of the reference frames used for the measurements in this manuscript can be found in Rosenheim et al. (2013).

During the measurements of calcite samples, at Tulane, two Carrara marble standards (IAEA CO-1 and IAEA Carbonate C1) and one internal coral standard (a mixture of coral rubble from Hawaii, CORS) were measured along with calcite samples at regular intervals. Each sample (calcite, Carrara marble standard, or CORS) was measured using 24 acquisitions, where each acquisition has 12 reference gas/sample gas changeovers with 12 seconds of changeover delay and 20 s of integration time. The reported Δ_{47} values are normalized to 25 °C phosphoric acid digestion temperature by using an acid fractionation factor of $-0.00141‰\ °C^{-1}$ extrapolated from an acid digestion fractionation factor of 0.092‰ reported by Henkes et al. (2013) for differences between 25 and 90 °C. This adopted $-0.00141‰\ °C^{-1}$ value is also verified by the offset of measured Δ_{47} values for Carrara marble standard (IAEA carbonate C1) digested at 100 and 25 °C, respectively. It is important to note that several other studies use a fractionation factor of 0.08‰ (Passey et al., 2010) rather than 0.092‰ (Henkes et al., 2013); in order to compare the results in this paper to other results corrected using the Passey et al. (2010) fractionation factor, one must simply subtract 0.012‰ from values reported herein. Average internal standard error of Δ_{47} for calcite samples measured at Tulane is about 0.012‰ (Table 1) and standard error of external Δ_{47} for Carrara marble is about 0.006‰ based on 19 repeated measurements (Rosenheim et al., 2013). Repeated measurements yield an average Δ_{47} value of 0.391 ± 0.006 (1 s.e.) for the Carrara marble, which is indistinguishable from those from other laboratories (0.392 ± 0.007 (1 s.e.) at Caltech; 0.385 ± 0.005 (1 s.e.) at Harvard; 0.403 ± 0.006 (1 s.e.) at Johns Hopkins; 0.4000 ± 0.004 (1 s.e.) at Yale; Dennis et al., 2011). At Tulane, the mean and standard error of 21 measurements of CORS was 0.7374 ± 0.005 for a temperature of 21 ± 1.9 °C (Dennis et al., 2011, Eq. (9)) which is reasonable for zooxanthellate corals living in cool tropical waters (Saenger et al., 2012). Repeated measurements of calcium carbonate laboratory reference materials were also used to monitor evidence of contamination.

At UCLA, the absolute reference frame was developed by analyzing heated gases with different bulk isotope compositions as well as gases equilibrated with water at 25 °C. Gases with different bulk $\delta^{18}O$ and ^{13}C ratios in quartz ampoules are heated to 1000 °C for two hours and then quenched at room temperature. Both types of standard gases are then purified and analyzed using the same protocol as gases generated from carbonate samples. At UCLA, approximately two to four sample analyses and three standard analyses (both gas standards and carbonate standards) were performed each day.

For carbonates, the Δ_{47} values from UCLA are normalized to 25 °C using a 0.08‰ value from Passey et al. (2010). Uncertainties in reported Δ_{47} values and calculated temperatures include the propagated uncertainty in heated gas determination and in sample measurement (Huntington et al., 2009). We repeatedly ran a Carmel Chalk standard and determined an average Δ_{47} value of $0.683 \pm 0.005‰$ (1 s.e.) at UCLA (compared to a nominal value of 0.697‰ based on analyses by Tripati at Caltech), a Carrera Marble standard with a value of $0.397 \pm 0.009‰$ (1 s.e.) (compared to a measured value of 0.397‰ from analyses at Caltech), and a TV01 standard with a value of $0.720 \pm 0.012‰$ (1 s.e.) (compared to a value of 0.713‰ measured at Caltech). Each of these standard values are on the absolute reference frame and use the Passey et al., 2010 acid digestion fractionation factor to normalize to 25 °C. Please note that, in order to make the Δ_{47} values for calcite samples measured at UCLA consistent with values from Tulane, all Δ_{47} values reported in Tables 1 and 2 are normalized to 25 °C using an acid fractionation factor of $-0.00141‰\ °C^{-1}$. Long-term precision as determined on replicate analyses of samples and standards is 0.005–0.009‰ (1 s.e.), equivalent to about 1–2 °C and consistent with other studies (Eiler, 2007; Huntington et al., 2009; Eagle et al., 2010, 2011, 2013; Tripati et al., 2010; Thiagarajan et al., 2011; Rosenheim et al., 2013). In order to monitor the presence of clean CO_2 samples, we screened for the presence of contaminating molecules such as hydrocarbons and sulfur compounds using mass 48 anomalies.

3. RESULTS

Comparison of isotopic data ($\delta^{13}C$, $\delta^{18}O$, and Δ_{47}) for inorganic calcites grown at 5 °C and measured in both laboratories (Table 2) shows that: (1) $\delta^{13}C$ and $\delta^{18}O$ data from both labs are consistent with each other; (2) differences between Δ_{47} values between samples measured in both labs are within analytical uncertainty; (3) the mean value of Δ_{47} for all 5 °C samples from each lab is identical (0.745 ± 0.005 at Tulane versus 0.751 ± 0.009 at UCLA); and (4) there is slightly more variability in the Δ_{47} data for each sample from Tulane versus UCLA, however the Tulane values spanned several different reference frames measured over a longer period of time (Rosenheim et al., 2013) whereas the UCLA samples were measured over a shorter period with an established stable reference frame.

Measured $\delta^{13}C$, $\delta^{18}O$, and Δ_{47} values of inorganic calcite precipitated at different temperatures, precipitation rates, pH, and ionic strengths are presented in Table 1. The data indicate that for the range of experimental conditions investigated in this study, temperature is significantly correlated

Table 1
Isotopic data ($\delta^{13}C$, $\delta^{18}O$, and Δ_{47}) for inorganic calcite spontaneously grown by the CO_2 diffusion technique. Data for growth temperature (T), pH, precipitation rate (R), and ionic strength (I) are from Tang et al. (2008, 2012).

T (°C)	Sample No.	Run No.[a]	log R (μmol/m^2/h)	pH	I (mM)	$\delta^{13}C$ (‰, VPDB)	$\delta^{18}O$ (‰, VSMOW)		Δ_{47} (‰, Absolute reference frame)		
							Each run	Each sample	Each run	Each sample	Each temperature
5	C50	237	1.89	8.3	35	−16.85	20.60	20.69	0.773 ± 0.008	0.754 ± 0.008	0.754 ± 0.006*
		444				−16.89	20.78		0.725 ± 0.013		
		UCLA-1				−16.87	20.62		0.757 ± 0.006		
		UCLA-2				−16.24	20.78		0.751 ± 0.014		
		UCLA-3				−16.75	20.65		0.765 ± 0.012		
	C26	241	2.84	8.3	35	−16.08	22.39	22.40	0.748 ± 0.012	0.753 ± 0.002	
		242				−15.99	22.40		0.746 ± 0.012		
		243				−16.04	22.42		0.750 ± 0.027		
		UCLA-2				−16.04	22.37		0.769 ± 0.008		
	C27	395	2.94	8.3	35	−18.99	21.61	21.52	0.742 ± 0.014	0.752 ± 0.009	
		396				−18.98	21.47		0.705 ± 0.012		
		398				−18.97	21.68		0.744 ± 0.013		
		UCLA-1				−18.99	21.48		0.767 ± 0.013		
		UCLA-2				−18.98	21.49		0.786 ± 0.009		
		UCLA-3				−18.99	21.41		0.767 ± 0.012		
	C48	205	2.96	8.3	35	−18.48	19.41	19.47	0.767 ± 0.008	0.759 ± 0.006	
		UCLA-1				−18.40	19.46		0.764 ± 0.009		
		UCLA-2				−18.35	19.51		0.748 ± 0.006		
		UCLA-3				−18.36	19.49		0.758 ± 0.009		
	C24	221	3.19	8.3	35	−18.74	22.05	22.12	0.778 ± 0.008	0.765 ± 0.014	
		427				−18.73	22.18		0.751 ± 0.013		
	C22	391	2.29	8.5	35	−15.09	22.49	22.42	0.787 ± 0.013	0.787 ± 0.001	
		393				−15.09	22.35		0.788 ± 0.012		
	C18	388	2.18	9.0	35	−19.09	17.42	17.37	0.738 ± 0.012	0.733 ± 0.019	
		389				−19.09	17.36		0.781 ± 0.013		
		390				−19.09	17.36		0.701 ± 0.014		
		UCLA-1				−19.10	17.33		0.713 ± 0.011		
	C19	207	2.25	9.0	35	−19.07	19.10	19.03	0.756 ± 0.007	0.735 ± 0.010	
		426				−19.03	19.07		0.712 ± 0.012		
		UCLA-1				−19.04	18.97		0.737 ± 0.008		
		UCLA-2				−19.04	18.98		0.734 ± 0.012		
	C20	UCLA-1	2.36	9.0	35	−17.94	19.41	19.39	0.748 ± 0.013	0.748 ± 0.007	
		UCLA-2				−18.01	19.37		0.737 ± 0.008		
		UCLA-3				−18.02	19.39		0.760 ± 0.009		
	C21	323	2.30	10	35	−18.61	4.32	4.33	0.946 ± 0.011	0.962 ± 0.006	
		380				−18.64	4.30		0.959 ± 0.012		
		381				−18.65	4.33		0.969 ± 0.015		
		384				−18.63	4.38		0.973 ± 0.012		
	C23	232	2.46	10.5	35	−19.43	2.85	2.89	1.080 ± 0.008	1.065 ± 0.008	
		324				−19.41	2.80		1.063 ± 0.013		
		377				−19.42	3.01		1.052 ± 0.013		

(*continued on next page*)

Table 1 (*continued*)

T (°C)	Sample No.	Run No.[a]	log R (μmol/m^2/h)	pH	I (mM)	$\delta^{13}C$ (‰, VPDB)	$\delta^{18}O$ (‰, VSMOW)		Δ_{47} (‰, Absolute reference frame)		
							Each run	Each sample	Each run	Each sample	Each temperature
25	C34	209	2.25	8.3	35	−19.39	18.39	18.47	0.711 ± 0.008	0.689 ± 0.011	0.688 ± 0.015
		420				−19.40	18.52		0.676 ± 0.012		
		452				−19.36	18.51		0.682 ± 0.0276		
	C32	204	3.02	8.3	35	−16.39	17.96	18.01	0.718 ± 0.009	0.710 ± 0.008	
		413				−16.44	18.06		0.703 ± 0.013		
	C30	234	3.57	8.3	35	−17.80	16.93	17.02	0.691 ± 0.009	0.706 ± 0.016	
		367				−17.74	17.06		0.756 ± 0.014		
		370				−17.75	16.95		0.662 ± 0.014		
		371				−17.74	17.07		0.721 ± 0.014		
		372				−17.74	17.07		0.701 ± 0.015		
	C29	210	4.21	8.3	35	−17.46	15.44	15.49	0.701 ± 0.010	0.684 ± 0.009	
		410				−17.44	15.53		0.681 ± 0.015		
		411				−17.44	15.49		0.671 ± 0.012		
	C58	230	1.92	8.3	292	−17.79	18.38	18.45	0.712 ± 0.008	0.698 ± 0.007	
		409				−17.78	18.45		0.689 ± 0.013		
		414				−17.78	18.52		0.694 ± 0.013		
	C57	405	2.18	8.3	292	−17.77	18.41	18.39	0.652 ± 0.014	0.657 ± 0.005	
		406				−17.77	18.36		0.662 ± 0.013		
	C54	400	3.38	8.3	292	−17.27	18.21	18.26	0.664 ± 0.013	0.670 ± 0.015	
		402				−17.27	18.28		0.648 ± 0.013		
		403				−17.27	18.28		0.697 ± 0.015		
40	C45	208	2.31	8.3	35	−21.72	15.92	15.89	0.632 ± 0.008	0.648 ± 0.015	0.649 ± 0.008
		450				−21.71	15.86		0.663 ± 0.015		
	C12	223	2.69	8.3	35	−16.76	15.18	15.19	0.682 ± 0.008	0.671 ± 0.014	
		224				−16.77	15.17		0.688 ± 0.009		
		225				−16.73	15.20		0.644 ± 0.010		
	C44	211	4.2	8.3	35	−12.57	14.91	14.91	0.630 ± 0.008	0.630 ± 0.008	
	C15	229	1.85	8.5	35	−14.13	14.87	14.97	0.647 ± 0.008	0.617 ± 0.030	
		423				−14.10	15.06		0.588 ± 0.012		
	C6	202	2.97	9.0	35	−21.01	13.67	13.68	0.642 ± 0.009	0.661 ± 0.019	
		415				−20.97	13.70		0.679 ± 0.012		
	C9	238	3.24	9.0	35	−17.22	11.92	11.92	0.643 ± 0.010	0.643 ± 0.010	
	C7	422	3.29	9.0	35	−16.30	11.61	11.47	0.670 ± 0.012	0.670 ± 0.001	
		430				−16.35	11.33		0.671 ± 0.013		

Note: All ±values are standard error $\left(\frac{\sigma}{\sqrt{n}}\right)$.

All Δ_{47} values are reported after applying an acid fractionation factor of −0.00141‰ °C^{-1}. If an acid fractionation factor of 0.08‰ for the 90–25 °C offset is used, a value of 0.012 should be subtracted from all Δ_{47} values in the table.

[a] nnn is the run number at Tulane and UCLA-n is the run number for each sample at UCLA.

[*] For average Δ_{47} values at 5 °C, only those calcite samples grown at pH ⩽9.0 are used.

Table 2
Comparison of isotopic data ($\delta^{13}C$, $\delta^{18}O$, and Δ_{47}) for inorganic calcite grown at 5 °C at Tulane and UCLA.

Sample No.	$\delta^{13}C$ (‰, VPDB)		$\delta^{18}O$ (‰, VSMOW)		Δ_{47} (‰, ARF)					
	Tulane	UCLA	Tulane	UCLA	Tulane			UCLA		
					Run	Sample	Mean	Run	Sample	Mean
C18	-19.09 ± 0.005	-19.10 ± 0.022	17.42 ± 0.126	17.33 ± 0.040	0.738 ± 0.012	0.759 ± 0.023	0.745 ± 0.005	0.713 ± 0.011	0.713 ± 0.011	0.751 ± 0.009
	-19.09 ± 0.007		17.36 ± 0.039		0.781 ± 0.013					
	-19.09 ± 0.006		17.36 ± 0.009		0.701 ± 0.014					
C19	-19.07 ± 0.008	-19.04 ± 0.003	19.10 ± 0.025	18.97 ± 0.007	0.756 ± 0.007	0.734 ± 0.022		0.737 ± 0.008	0.736 ± 0.002	
	-19.03 ± 0.008	-19.04 ± 0.004	19.07 ± 0.153	18.98 ± 0.011	0.712 ± 0.012			0.734 ± 0.012		
C26	-16.08 ± 0.005	-16.04 ± 0.002	22.39 ± 0.012	22.37 ± 0.007	0.748 ± 0.012	0.748 ± 0.001		0.769 ± 0.008	0.769 ± 0.008	
	-15.99 ± 0.005		22.40 ± 0.010		0.746 ± 0.012					
	-16.04 ± 0.005		22.42 ± 0.011		0.750 ± 0.027					
C27	-18.99 ± 0.005	-18.99 ± 0.002	21.61 ± 0.046	21.48 ± 0.002	0.742 ± 0.014	0.730 ± 0.013		0.767 ± 0.013	0.773 ± 0.007	
	-18.98 ± 0.008	-18.98 ± 0.003	21.47 ± 0.071	21.49 ± 0.003	0.705 ± 0.012			0.786 ± 0.009		
	-18.97 ± 0.014	-18.99 ± 0.004	21.68 ± 0.153	21.41 ± 0.006	0.744 ± 0.013			0.767 ± 0.012		
C48	-18.48 ± 0.005	-18.40 ± 0.002	19.41 ± 0.023	19.46 ± 0.009	0.767 ± 0.008	0.767 ± 0.008		0.764 ± 0.009	0.757 ± 0.005	
		-18.35 ± 0.002		19.51 ± 0.006				0.748 ± 0.006		
		-18.36 ± 0.021		19.49 ± 0.026				0.758 ± 0.009		
C50	-16.85 ± 0.004	-16.87 ± 0.003	20.60 ± 0.009	20.62 ± 0.007	0.773 ± 0.008	0.749 ± 0.024		0.757 ± 0.006	0.758 ± 0.004	
	-16.89 ± 0.030	-16.24 ± 0.003	20.78 ± 0.178	20.78 ± 0.005	0.725 ± 0.013			0.751 ± 0.014		
		-16.75 ± 0.002		20.65 ± 0.009				0.765 ± 0.012		

Note: All ±values for $\delta^{13}C$, $\delta^{18}O$ are standard deviation (σ) and for Δ_{47} are standard error $\left(\frac{\sigma}{\sqrt{n}}\right)$.

All Δ_{47} values are reported after applying an acid fractionation factor of $-0.00141‰\ °C^{-1}$. If an acid fractionation factor of 0.08‰ for the 90–25 °C offset is used, a value of 0.012 should be subtracted from all Δ_{47} values in the table.

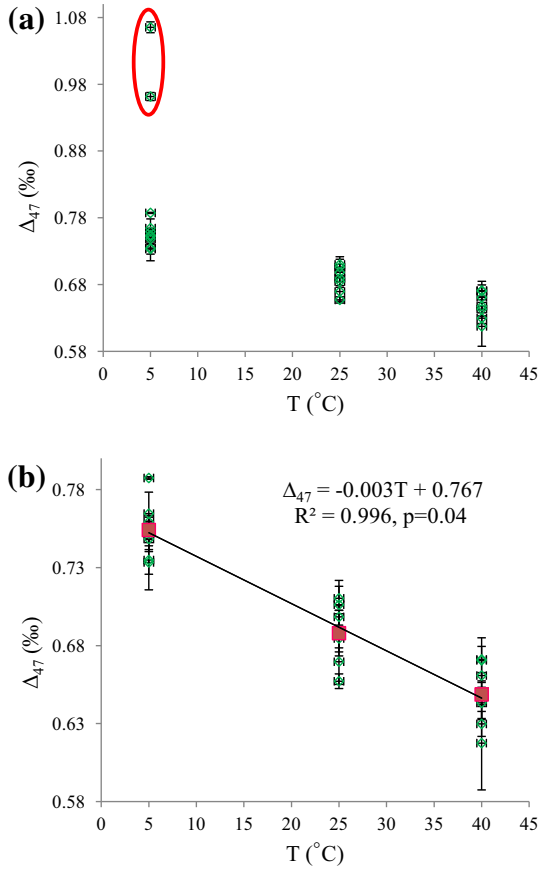

Fig. 2. (a) Average Δ_{47} value for each inorganic calcite sample versus its growth temperature (T); (b) Average Δ_{47} value for each inorganic calcite sample grown at pH $\leqslant$9.0 versus its growth temperature. Data points in red circle are calcite grown at pH $\geqslant$10. Green diamond is average Δ_{47} value for each sample. Red square is average Δ_{47} value for each temperature. The black line is linear regression through average Δ_{47} values at each temperature. Regression equation, *R*-squared value, and *p*-value are also reported on chart. (For interpretation of the references to colour in this figure legend, the reader is referred to the web version of this article.)

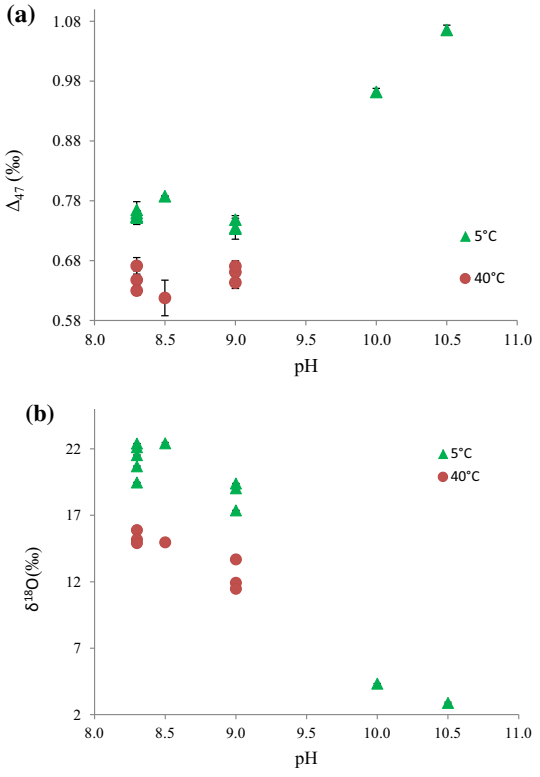

Fig. 3. Average (a) Δ_{47} and (b) $\delta^{18}O$ value for each inorganic calcite sample versus growth pH.

with Δ_{47}, pH may be correlated with Δ_{47}, but precipitation rate and ionic strength are relatively unimportant. When the average Δ_{47} measured for each calcite sample is plotted against its growth temperature (Fig. 2a), it is evident that measured Δ_{47} values generally decrease with increasing temperatures, consistent with previous studies. Two calcite samples grown at pH $\geqslant$10 (Fig. 2a) measured at Tulane deviate from the observed correlation and have substantially higher measured Δ_{47} values. Fig. 2b shows a linear regression through the average values for all samples, excluding the two samples grown at high pH. Whereas pH seems to relate to $\delta^{18}O$ variability (Fig. 3b), no significant correlation between Δ_{47} and pH is observed in the Tulane data until a threshold (between pH 9 and pH 10) is exceeded (Fig. 3a). At all temperatures of precipitation, Δ_{47} does not covary with precipitation rate (Fig. 4), even when temperature, pH, and ionic strength are held constant. Again, two high-pH values stand out as outliers (samples grown at 5 °C, Fig. 4). The increase of ionic strength from 35 to 292 mM shows no effect on Δ_{47} (Fig. 4b). The $\delta^{18}O$ values seem to be insensitive to precipitation rate at 5 °C, but decrease with increasing precipitation rates at 25 and 40 °C when other parameters (e.g., pH, temperature, and ionic strength) are held constant (Fig. 5). The $\delta^{18}O$ values are more sensitive to variation in precipitation rate at a lower ionic strength (Fig. 5b) or at a higher pH (Fig. 5c).

4. DISCUSSION

4.1. Comparison of results for Δ_{47} with $\delta^{18}O$

In general, our data illustrate that under the conditions that these synthetic samples were precipitated, clumped isotopes are less sensitive to physicochemical parameters (e.g., pH, the precipitation rate, and ionic strength) than oxygen isotopes. Fig. 3 shows that Δ_{47} only responds to variation in pH at high pH range (pH $\geqslant$10), whereas $\delta^{18}O$ seems to respond to the change of pH over the whole pH range. However, we must point out that, statistically, the $\delta^{18}O$–pH relationship at low pH range is rather uncertain, which indicates that $\delta^{18}O$ may not vary with pH $\leqslant$9 in our experiments either.

There is no demonstrable influence of precipitation rate on Δ_{47} values reported herein (Fig. 4), where precipitation rates were more or less consistent with those reported for natural systems (Table 3). All Δ_{47} values measured at Tulane are insensitive to variable precipitation rates, even

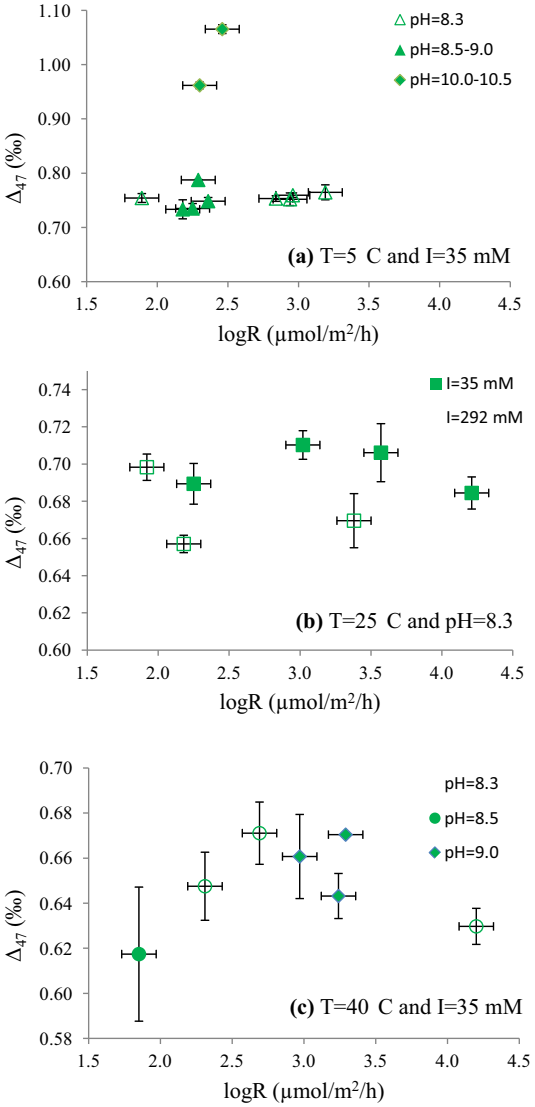

Fig. 4. Average Δ_{47} value for each inorganic calcite sample versus precipitation rate: (a) $T = 5$ °C; (b) $T = 25$ °C; and (c) $T = 40$ °C.

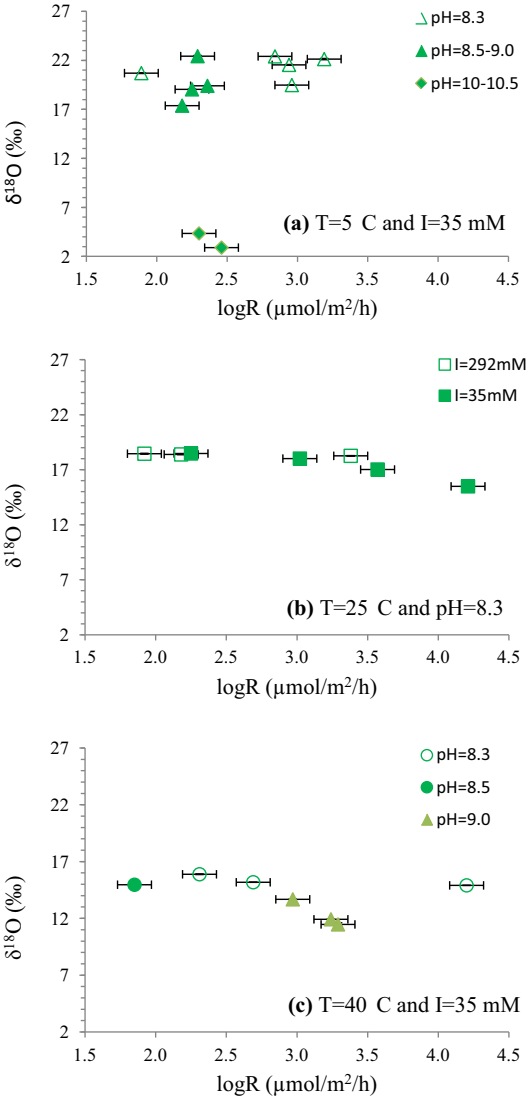

Fig. 5. Average $\delta^{18}O$ value for each inorganic calcite sample grown at 25 °C versus precipitation rate.

when temperature, growth pH, and ionic strength are held constant (Fig. 4). Fig. 5 shows that, at 25 and 40 °C, when growth pH and ionic strength are held constant, $\delta^{18}O$ values for inorganic calcite are negatively correlated to the precipitation rate. This is in contrast to the Δ_{47} data presented in Fig. 4b and c. Data presented in Figs. 4b and 5b show that variations in ionic strength also affect oxygen isotopes but not clumped isotopes. As shown in Fig. 4b, increasing the ionic strength from 35 to 292 mM has no impact on measured Δ_{47} values. In contrast, Fig. 5b shows that $\delta^{18}O$ value is more sensitive to the precipitation rate for calcite grown at ionic strength of 35 mM than grown at ionic strength of 292 mM, which indicates that variation in ionic strength will also influence oxygen isotope composition. Thus, using our precipitation method, variations in precipitation rate apparently only influence oxygen isotope composition and not clumped isotope composition within current measurement precision of Δ_{47}.

4.2. The influence of pH on $\delta^{18}O$ and Δ_{47}

Two calcite samples grown from solutions with a high pH (pH $\geqslant$ 10) that were measured at SILT-U have significantly distinct Δ_{47} values from other samples grown at the same temperature. A small difference in Δ_{47} values is observed in the UCLA data for 5 °C samples that are grown at pH 8.3 and 9.0. It is well know that the distribution of DIC species is pH-dependent. Additionally, the time to attain isotopic equilibrium between DIC species and water is pH-dependent (Usdowski et al., 1991; Beck et al., 2005). Therefore, pH may influence oxygen and clumped isotopes through two ways: (1) equilibrium DIC speciation and (2) CO_2 hydration and hydroxylation.

4.2.1. DIC speciation as a cause for bulk and clumped isotope fractionation

In the case of the DIC speciation, the distribution of DIC species (i.e., CO_2 (aq), H_2CO_3, HCO_3^-, and CO_3^{2-}) is

Table 3
Typical calcification and precipitation rates (R) for natural calcium carbonates.

Sample	Estimated R (μmol/m^2/h)	log R	Reference
Inorganic calcite	63–25119	1.8–4.4	Tang et al. (2008)
Planktonic and benthonic foraminifera	35–4300	1.54–3.63	Carpenter and Lohmann (1992)
Sclerosponge (*C. nicholsoni*)	310	2.49	Gussone et al. (2005)
Sclerosponge (*A. wellsi*)	630	2.80	
Foraminifera (*O. universa*)	2417	3.38	Saenger et al. (2012)
Mollusks	667–1667	2.82–3.20	
Corals	1500–22,167	3.18–4.35	
Corals	9000–25,000	3.95–4.40	Gaetani et al. (2011)
Speleothems*	619–5414	2.78–3.73	Daëron et al. (2011)
Speleothems*	40–4640	1.6–3.67	Kluge and Affek (2012)
Speleothem (plate experiment in Bahamas cave)	46–1140	1.66–3.06	Arienzo et al. (2013)

* Precipitation rate for speleothem was estimated from growth rate by assuming the density of speleothem is 2.71 g/cm^3.

pH-dependent. In general, the dominant DIC species is CO_2 (aq) at low pH range (<6.0), HCO_3^- at intermediate pH range (6.0–9.5), and CO_3^{2-} at high pH range (>9.5), although the specific pH range may vary with solution composition as well as temperature. Previous studies (Usdowski et al., 1991; Beck et al., 2005) have demonstrated that, at isotopic equilibrium, $\delta^{18}O$ values of DIC species decrease in the sequence of CO_2(aq), H_2CO_3, HCO_3^-, and CO_3^{2-}. For equilibrium clumped isotope composition in DIC species, it is predicted that Δ_{47} is lower following the same sequence based on experimental $BaCO_3$ precipitation (Tripati et al., in revision) and theoretical calculations (Tripati et al., in revision; Guo, 2008; Hill et al., 2013). For example, when DIC species are isotopically equilibrated with water at 25 °C, Tripati et al. (in revision) reported that CO_3^{2-} may be about 0.06‰ lower in Δ_{47} than HCO_3^- based on quasi-instantaneous precipitation as $BaCO_3$, whereas Hill et al. (2013) and Tripati et al. (in revision) predicted that Δ_{47} value of CO_3^{2-} is ~0.02–0.03‰ lower than Δ_{47} value of HCO_3^-. Tripati et al. (in revision) predicted a positive Δ_{47}-$\delta^{18}O$ slope of 0.004–0.011 arising from DIC speciation effects.

If inorganic calcite grows rapidly from a mixture of DIC species in proportion to their aqueous species ratios as hypothesized by Zeebe (1999) and Tripati et al. (in revision), then pH can influence oxygen ($\delta^{18}O$) and clumped isotopes (Δ_{47}) in calcite through DIC speciation. However, over a range of growth rates, these models and the model of DePaolo (2011) suggest that DIC speciation effects may not be recorded by growing crystals. For our calcite samples grown at pH ⩽9.0, Δ_{47} data show variability that is wholly unrelated to variation in pH (Fig. 3a). It is possible that the range of growth rates sampled may not be sufficiently high for DIC speciation effects to be recorded, however the growth rates employed in our experiments are generally comparable to those found in nature (Table 3).

A caveat is that for the one sample set that was analyzed in both labs (samples that were grown at 5 °C), mean values and variability are similar, but slightly different trends are observed with pH. A statistically significant difference between samples grown at pH values of 8.3 and 9.0 in both Δ_{47} and $\delta^{18}O$ is observed in measurements from UCLA that is consistent with the direction of change expected due to DIC speciation effects (Tripati et al., in revision; Hill et al., 2013). For this subset of samples, no trend with pH is observed in the dataset generated at Tulane, which could reflect a small difference between these samples relative to analytical precision.

At high pH values in our data set, the opposite direction of the response of Δ_{47} and $\delta^{18}O$ to variation in pH implies that other kinetic factors (e.g., diffusion through the membrane and CO_2 hydroxylation, as discussed in more detail below) may be important in these samples. The DIC speciation effect cannot account for kinetic oxygen and clumped isotope fractionation observed in these inorganic synthetic calcites. If an equilibrium DIC speciation effect was the sole factor influencing these samples, we would predict that both Δ_{47} and $\delta^{18}O$ would exhibit smaller values at higher pH because both Δ_{47} and $\delta^{18}O$ values in DIC species become smaller following the sequence of CO_2(aq), H_2CO_3, HCO_3^-, and CO_3^{2-} (Tripati et al., in revision) and the percentage of HCO_3^-, and CO_3^{2-} increases with pH. In contrast, we observe larger Δ_{47} and smaller $\delta^{18}O$ values (negative slope) for two calcite samples grown at pH ⩾ 10 when compared to those grown at pH ⩽ 9.0 (Fig. 3).

4.2.2. CO_2 diffusion through the membrane and CO_2 hydroxylation as a cause for bulk and clumped isotope fractionation

Isotopic equilibration times for DIC species with water are both temperature- and pH-dependent, with longer times reported for low temperatures and for high pH values (Usdowski et al., 1991; Beck et al., 2005; Geisler et al., 2012). In solutions, not only is the distribution of DIC species pH-dependent, but the isotopic equilibration time for DIC species with water is also pH-dependent (Usdowski et al., 1991; Beck et al., 2005; Geisler et al., 2012). Therefore it is possible that high pH and/or low temperatures can also cause kinetic isotope effects in both bulk compositions and clumped isotope compositions. For example, Beck et al. (2005) reported that at pH 8.0–8.7, the time for isotopic equilibration of DIC species with water was about 2 h at 40 °C and 24 h at 15 °C, whereas at pH >11, isotopic equilibration time for DIC species increased to 270 h at 40 °C and was more than 2640 h at 15 °C. For our inorganic calcite precipitation, the waiting time after CO_2 crosses the membrane and before the first calcite precipitation occurred was 120–456 h at 5 °C. Increasing the pH to 10 shortens waiting time to 120 h and pH 10.5 yields a waiting time

of 48 h. At 40 °C, waiting times range between 2 and 264 h for low pH experiments (pH ⩽9.0)(Tang et al., 2008). Thus, DIC species may reach isotopic equilibrium with water at low pH range (pH ⩽9.0), because the waiting time for DIC species is longer than isotopic equilibrium time in the solution. But at high pH range (pH ⩾10.0) they may not reach equilibrium due to insufficient waiting time for DIC species to exchange isotopes with water. This argument can also be supported by our observation that both $\delta^{18}O$ and Δ_{47} apparently respond to variation in pH at the high pH range but show a very weak relationship with high uncertainty (i.e., $\delta^{18}O$) or no relationship (i.e., Δ_{47}) with pH at the low pH range.

Under conditions of isotopic disequilibrium in the solution, two possible processes can cause kinetic isotopic fractionation in our experiments: (1) diffusion through the membrane and (2) CO_2 hydroxylation. Thiagarajan et al. (2011) discussed the effects of diffusion across a lipid bilayer, through a gas phase, or in an aqueous medium on $\delta^{18}O$ and Δ_{47}. Although we do not understand how diffusion through a polyethylene membrane affects $\delta^{18}O$ and Δ_{47} values of CO_2, according to Thiagarajan et al. (2011), it is expected that CO_2 that diffusing through the membrane should have a larger Δ_{47} value and smaller $\delta^{18}O$ value. In our experiments, CO_2 that crosses the membrane redissolves in the $CaCl_2$ solution. If DIC species have not attained isotopic equilibrium with water before calcite precipitates, the diffusive signal of $\delta^{18}O$ and Δ_{47} would be inherited by calcite. Therefore, the smaller $\delta^{18}O$ values and larger Δ_{47} values that are observed in those calcite samples grown at high pH values might be caused by diffusion through the membrane. Under isotopic disequilibrium conditions, kinetic isotope fractionation associated with CO_2 hydroxylation might also lead to smaller $\delta^{18}O$ values and larger Δ_{47} values. According to the studies of McConnaughey (1989), CO_2 hydration and hydroxylation preferentially select light isotopes ^{12}C and ^{16}O and discriminate against heavy isotopes ^{13}C and ^{18}O. As a result, $\delta^{13}C$ and $\delta^{18}O$ are depleted in DIC species and thus in calcite from which it precipitates. Although, to date, there are no published references to how CO_2 hydration and hydroxylation influence clumped isotopes, Daëron et al. (2011) suggest that HCO_3^- dehydration and dehydroxylation may kinetically increase $\delta^{13}C$ and $\delta^{18}O$ but decrease Δ_{47} in the residual aqueous HCO_3^- species and thus in calcium carbonate from which it grows, supported by theoretical calculations from Guo (2008) using transition state theory. Speleothem data show that a 1‰ kinetic enrichment in $\delta^{18}O$ will correspond to about 0.05–0.06‰ kinetic depletion in Δ_{47}. Based on McConnaughey's (1989) and by extending Daëron et al. (2011) and Guo's (2008) studies examining isotopic fractionations associated with CO_2 dehydration and dehydroxylation, it is plausible that the reverse processes – CO_2 hydration and hydroxylation – may lead to kinetic depletion in $\delta^{18}O$ and enrichment in Δ_{47}. A similar argument was also proposed by Saenger et al. (2012) to interpret negative $\delta^{18}O$ and positive Δ_{47} offsets observed in their coral samples. Using the data presented in Fig. 6, we calculate that $\frac{\text{average}\Delta_{47,\text{high pH}}-\text{average}\Delta_{47,\text{low pH}}}{\text{average}\delta^{18}O_{\text{high pH}}-\text{average}\delta^{18}O_{\text{low pH}}}=-0.016$, which indicates that Δ_{47} values increase about 0.016‰ for every 1‰ decrease in $\delta^{18}O$ ratio when pH increases from low pH range (DIC isotopic equilibrium) to high pH range (DIC isotopic disequilibrium). The kinetic enrichment in Δ_{47} versus kinetic depletion in $\delta^{18}O$ observed in our inorganic calcite (produced by CO_2 diffusion and re-dissolving) is smaller than what was reported from speleothems (i.e., −0.01) in Daëron et al. (2011) and the Guo (2008) model prediction (i.e., $-0.017 \sim -0.026$) of the kinetic depletion in Δ_{47} versus kinetic enrichment in $\delta^{18}O$ during CO_2 degassing. Therefore, part of kinetic effects of diffusion through the membrane and CO_2 hydroxylation must have been offset by other processes such as DIC-water isotope exchange. Further theoretical and experimental work is needed to investigate kinetic isotope effects associated with CO_2 diffusion through the membrane and CO_2 hydration and hydroxylation.

Dietzel et al. (2009) proposed that non-equilibrium $\delta^{18}O$ for inorganic calcite is controlled by the combination of isotopic non-equilibrium of DIC species in the solution phase and isotopic disequilibrium in newly formed calcite crystals due to the entrapment of "^{18}O-depleted" surface layer into crystal lattice. As a result, even when DIC species have attained isotopic equilibrium with water, oxygen isotopes are still influenced by the precipitation rate, because fast precipitation will result in more effective entrapment of the "^{18}O-depleted" surface layer into the crystal lattice (see Watson, 2004; Dietzel et al., 2009). The new data presented in this study further confirm that $\delta^{18}O$ would be influenced by both isotope disequilibrium processes, whereas Δ_{47} might be only influenced by isotope disequilibrium in the solution. It is possible that these data reflect that Δ_{47} in the mineral can reach equilibrium more readily than $\delta^{18}O$.

Currently we cannot exclude there is a surface entrapment mechanism for clumped isotopes. Although we do not directly test that hypothesis here, these data provide constraints for future modeling studies of the growth entrapment model over the range of growth rates and experimental conditions sampled. Any model would need to match the following observations: (1) there is a clear pH effect on both $\delta^{18}O$ and Δ_{47} values at pH ⩾10 where DIC is slow to attain isotopic equilibrium with water; (2)

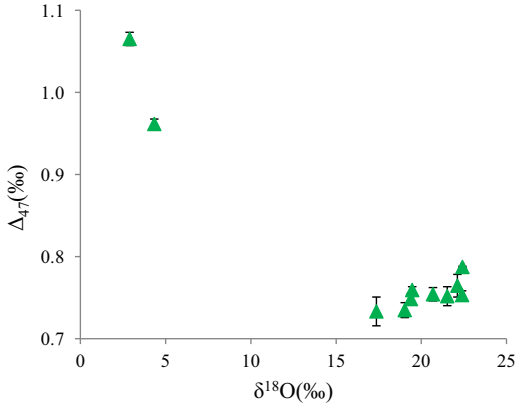

Fig. 6. Average Δ_{47} value for each inorganic calcite sample grown at 5 °C versus its $\delta^{18}O$ value.

there are no clear effects of pH on both $\delta^{18}O$ and Δ_{47} values at pH $\leqslant$9.0; (3) there are no effects of precipitation rate and ionic strength on Δ_{47} over the experimental conditions sampled, but these effects are apparent on $\delta^{18}O$ at pH $\leqslant$9.0; (4) Δ_{47} values increase and $\delta^{18}O$ values decrease when pH increases from low pH range (DIC isotopic equilibrium) to high pH range (DIC isotopic disequilibrium), which is consistent with kinetic isotopic fractionation associated with diffusion as well as CO_2 hydroxylation.

4.3. Equilibrium Δ_{47} values

When pH $\leqslant$9.0, precipitation rate, pH, and ionic strength have little to no effect on clumped isotopes (see Figs. 3 and 4), but have significant effects on $\delta^{18}O$ (Fig. 5). The $\delta^{18}O$ values in our experiment lie systematically below the Coplen (2007) "equilibrium" line (Fig. 7) as well as the commonly adopted Kim and O'Neil (1997) "equilibrium" line. Equilibrium oxygen isotope fractionation was not easily attained during inorganic calcite precipitation in our experiments (Dietzel et al., 2009) (Fig. 7). Even for those calcites grown slowly from laboratory experiments, precipitation rate-related $\delta^{18}O$ variations were still observed when both temperature and pH are held constant (see Dietzel et al., 2009 for details). In contrast, our measured Δ_{47} values for inorganic calcite are apparently sensitive principally to temperature, with a threshold-type response to high pH (i.e., at some pH where isotopic equilibrium time in the solution is equal to the waiting time for DIC species). If all of our samples are not in equilibrium, the implication is that kinetic isotope effects exist in Δ_{47} but cannot be measured with current precision of the clumped isotope method, whereas such effects can be measured with higher analytical precision in $\delta^{18}O$.

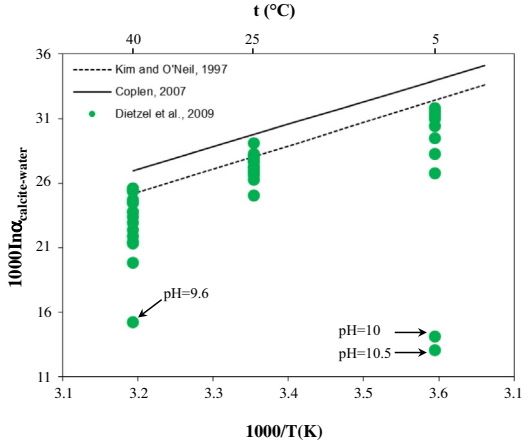

Fig. 7. Plot of $1000\ln\alpha_{calcite-water}$ in this data set compared to proposed "equilibrium" lines. Most of the $1000\ln\alpha_{calcite-water}$ values are below the Kim and O'Neil (1997) line and all values yield a smaller $1000\ln\alpha_{calcite-water}$ than would be expected by the Coplen (2007) line. Low outliers from the data set include all samples analyzed at an elevated pH. This plot depicts the full data set of Dietzel et al. (2009); only a subset of samples was analyzed for Δ_{47} in this project. The high temperature, high pH sample did not have enough material for replicated Δ_{47} measurements and was not included in our work.

The variance in Δ_{47} values at each temperature (Fig. 2b) may be related to the variability in the precipitation parameters such as pH, precipitation rate, and ionic strength, but our inability to relate these parameters to trends in the data (Figs. 3a and 4) may simply be related to present constraints on the precision of Δ_{47} measurements. However, the fact that we see no pH effect on Δ_{47} or a very weak pH effect with high uncertainty on $\delta^{18}O$ at low pH range as well as the long waiting time for DIC species in our experiments implies that precipitation rate- and ionic strength-related kinetic effects on oxygen isotopes are mainly due to preferential entrapment of ^{16}O during calcite formation.

It is possible the Δ_{47} data may indicate that thermodynamic equilibrium is attained in Δ_{47} more readily than in $\delta^{18}O$ in carbonate minerals because of the effects of surface entrapment on $\delta^{18}O$, although Affek (2013) showed that both Δ_{47} and $\delta^{18}O$ approached equilibrium values at the same rate in the reaction of CO_2 hydration/dehydration for one set of conditions. If we assume calcite grown during our experiments did not achieve equilibrium $\delta^{18}O$ values but do approximate equilibrium Δ_{47} values (excluding the two high pH samples at 5 °C) due to differences in the timescale for equilibration, then we derive the following Δ_{47}-temperature calibration using average sample values for each temperature:

$$\Delta_{47} = (0.0387 \pm 0.0072) \times 10^6/T^2 + (0.2532 \pm 0.0829) \quad (r^2 = 0.9998, p = 0.009).$$

This uses an acid digestion fractionation factor of 0.092‰ for the 90–25 °C offset from Henkes et al. (2013). The intercept of this equation changes to 0.2412 ± 0.0829 if an acid fractionation factor of 0.08‰ between 90 and 25 °C (Passey et al., 2010). The Δ_{47}-temperature calibration derived from our data (Fig. 7) is indistinguishable from theoretical calculations for calcite (Eq. (4) of Passey and Henkes, 2012), which are based on first-principles modeling (Schauble et al., 2006) and combined with an experimental acid fractionation factor of 0.268‰ on the absolute reference frame. The slope of our calibration line is also similar to theoretical calculations for calcite (Hill et al., 2013) using supermolecular cluster models. The first empirical calibration to demonstrate reduced temperature sensitivity (shallower slope) of Δ_{47} was Dennis and Schrag (2010). Similar to their calibration, the slope of our line is shallower than the calibration of Ghosh et al. (2006) when projected into the absolute reference frame (Fig. 8). In previous work, two observations have been used to interpret Δ_{47} values as kinetically driven, rather than representing equilibrium values: (1) comparison of the slope to inorganic calcite calibrations and (2) comparison to oxygen isotope disequilibrium (Affek et al., 2008; Daëron et al., 2011; Kluge and Affek, 2012; Dennis et al., 2013). Based on the lack of a measurable influence of kinetic fractionation drivers (precipitation rate, ionic strength) on measured Δ_{47} in this study, it is possible that the our Δ_{47}-temperature calibration nominally represents equilibrium precipitation, where DIC species have attained isotopic equilibrium with water and disequilibrium $\delta^{18}O$ values are mainly due to preferential entrapment of ^{16}O into calcite crystal. In this case, and until Δ_{47}

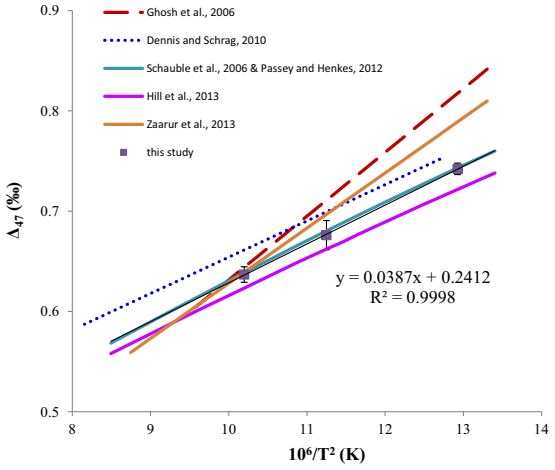

Fig. 8. Comparison of these results with published data from inorganic synthetic calcite, as well as theoretical calculations. Black solid line is linear regression through averages of our data at each temperature (purple squares with error bars – 1 s.e.). Regression equation, *R*-squared value, and *p*-value are also reported on chart. To facilitate comparison with other studies, in this figure, our data were reported with an acid digestion fractionation factor of 0.08‰ for the 90–25 °C offset from Passey et al. (2010).(For interpretation of the references to colour in this figure legend, the reader is referred to the web version of this article.)

measurements become more precise, it may be more parsimonious to identify kinetic Δ_{47} effects more directly using responses to pH, precipitation rate, and water chemistry when feasible.

4.4. Implication for Δ_{47}-temperature calibration discrepancies

The temperature sensitivity of our Δ_{47} calibration data is consistent with a body of published work that yield a shallower slope (Dennis and Schrag, 2010; Dennis et al., 2013; Eagle et al., 2013; Henkes et al., 2013). Here, we evaluate the discrepancy of Δ_{47}-temperature calibrations and the recent increase in reports of reduced sensitivity of Δ_{47} to temperature in terms of both analytical methods and methods of synthesis of carbonates:

(1) analytical methods

Calibration discrepancies might be due to different analytical methods adopted by different laboratories. Fernandez et al. (2014, see Fig. 7 therein) compiled published Δ_{47} data digested at different temperatures and found that Δ_{47} data digested at high temperatures (70–100 °C) fell into a linear regression line with a shallow slope similar to Dennis and Schrag (2010) calibration slope, whereas Δ_{47} data digested at low temperature (25 °C) followed a linear regression line with a relative steep slope similar to Ghosh et al. (2006) calibration slope. Fernandez et al. (2014) further proposed that different acid digestion methods might result in different clumped isotope acid fractionation factors, a topic discussed in depth at the 3rd International Clumped Isotope Workshop held in Boston, Massachusetts, USA (Harvard University) in January, 2013. The difference in the vapor pressure of water as a function of temperature might promote isotopic exchange between CO_2 and water at higher temperatures, which can also cause calibration discrepancies at different acid digestion temperatures. Eagle et al. (2013) suggested that samples with different isotopic composition may have different the clumped isotope acid fractionation factors and may have different effect on clumped isotopes during sample gas purification. Systematic studies are required to understand the effects of isotopic composition and acid digestion temperature on clumped isotope acid fractionation factor, and our data support the need for such studies to elaborate on these calibration differences.

(2) methods of synthesis

Physicochemical parameters (high pH, low temperature, fast precipitation) or physical processes (CO_2 degassing or absorption, CO_2 diffusion, mixing of solution) may result in DIC isotopic disequilibrium and thus produce disequilibrium Δ_{47} values in carbonates. Therefore, carbonate growth environments or growth techniques are important for clumped isotopes to reach isotopic equilibrium. In the experiments of Ghosh et al. (2006), inorganic calcite was synthesized using an active degassing method (i.e., CO_2 was removed by purging N_2 gas through a Ca^{2+} and HCO_3^- rich solution), whereas in Dennis and Schrag (2010) experiments, inorganic calcite was precipitated using a passive degassing method (i.e., Ca^{2+}–HCO_3^- solution was open to the atmosphere and CO_2 passively degases). Different synthetic methods might contribute some calibration discrepancy between the calibration lines for synthetic carbonates. Since both Ghosh et al. (2006) and Dennis and Schrag (2010) did not control pH and the precipitation rate in their experiments, it is difficult to assess whether their isotopic data are correlated with these variables and infer which experiments more closely approach isotopic equilibrium. However, in experimental setups of Ghosh et al. (2006) as well as Dennis and Schrag (2010), pH is expected to vary between 7.0 and 9.0. Based on our data at low pH range (pH $\leqslant$9.0), clumped isotopes readily approach equilibrium in calcite. The waiting time for precipitation from Ca^{2+}–HCO_3^- solution in Ghosh et al. (2006) experiments was reported to be typically about 1 day, which is sufficient to allow DIC to exchange isotopes with water (Beck et al., 2005). Although passive degassing in Dennis and Schrag (2010) experiments might cause DIC disequilibrium, DIC species in their experiments are expected to approach isotopic equilibrium with water because the mixture of $CaCl_2$ solution and the $NaHCO_3$ solution was continuously stirred and precipitation is relatively slow (1–4 days, dependent on experimental temperature).

We conclude that discrepancies between original steeper calibrations and more recent shallower calibrations are likely due to analytical methods rather than methods of mineral synthesis based on our findings in this experiment. Based on our observation that Δ_{47} more readily approaches equilibrium than $\delta^{18}O$ for slow laboratory carbonate precipitation at low pH range (pH $\leqslant$9.0), it is reasonable to

suggest that both Ghosh et al. (2006) and Dennis and Schrag (2010) calibration can represent clumped isotope equilibrium. Recently, Zaarur et al. (2013) re-examined the original steep calibration with the same inorganic precipitation technique but a wider temperature range and higher analytical precision. Their results further confirmed that the original calibration can reflect clumped isotope equilibrium, however they performed their reactions at a lower temperature and both the biogenic carbonates and the laboratory-precipitated carbonates fell on a steeper line similar to Ghosh et al. (2006).

4.5. Implications for natural samples

At a precipitation rate range of $\log R = 1.8$–4.4 μmol/m^2/h and other experimental conditions sampled, we observe kinetic effects due to crystal growth on $\delta^{18}O$ but are not resolvable in our experimental Δ_{47} data. Table 3 lists typical calcification and precipitation rates for natural marine carbonates and speleothems obtained from references. It is important to note that estimated precipitation rates for most of natural marine carbonates fall into the precipitation rate range investigated in this study. Therefore, it is possible that kinetic effects due to crystal growth may be relatively unimportant on Δ_{47} in most natural marine samples, if they grow under similar conditions and by similar mechanisms. In addition, marine calcium carbonates grow from the solutions with pH slightly higher than regular freshwaters (typical pH of seawater is 8.3) and elevated ionic strength (typical ionic strength of seawater is 700 mM). At pH 8.3, our experiments show, when ionic strength increased from 35 to 292 mM, the measured Δ_{47} values show no difference but the measured $\delta^{18}O$ values are insensitive to variation in precipitation rate. These results imply that kinetic effects might be not important to both oxygen isotopes and clumped isotopes in natural marine carbonates due to elevated ionic strength.

Speleothems are typically formed in underground caves when CO_2 degases from karstic waters. The ionic strengths of karstic waters should be close to those of our low ionic strength experiments (i.e., 35 mM). The pH values of waters from which speleothems precipitate are reported to be 7.13–8.2 (Daëron et al., 2011). Our data may indicate that when DIC reaches isotopic equilibrium with water, Δ_{47} in carbonate minerals reflects an equilibrium value, but when DIC has not attained isotopic equilibrium with water, both $\delta^{18}O$ and Δ_{47} values are influenced by isotopic disequilibrium in the solution. Although natural speleothems fall into the precipitation rate range investigated in this study and their growth solutions have similar pH and ionic strengths as our experiments conducted at pH $\leqslant$9.0, kinetic effects are expected on both $\delta^{18}O$ and Δ_{47} in natural speleothems because they are actively degassing CO_2 which leads to isotopic disequilibrium in the solution.

5. SUMMARY

In this contribution, we present a set of Δ_{47} data measured from inorganic synthetic calcite produced by an advanced CO_2 diffusion technique. Because in our experiments temperature, pH, precipitation rate, and ionic strength are well-controlled, our data let us examine how clumped isotopes respond to multiple variables. Our new Δ_{47} data show, under the range of experimental conditions investigated in this study ($T = 5$–40 °C, $\log R = 1.8$–4.4 μmol/m^2/h, pH 8.3–10.5, and $I = 35$–832 mM) and using our experimental protocol, that:

(1) Clumped isotopes are relatively insensitive to pH at a low pH range (pH $\leqslant$9.0), but show a larger response to a variation in pH at high pH range (pH $\geqslant$10.0).
(2) With the data available and at the state-of-the-science instrumental resolution we have, we do not resolve any clear effects of precipitation rate and ionic strength on measured Δ_{47} which compare in magnitude to the effects on $\delta^{18}O$.
(3) Clumped isotopes are less sensitive to physicochemical parameters (e.g., pH, precipitation rate, ionic strength) than oxygen isotopes, which implies that at current analytical precision, clumped isotopes may more readily attain apparent isotopic equilibrium than oxygen isotopes.
(4) A $\Delta_{47}/\delta^{18}O$ slope of -0.016 is reported based on measurements of samples grown at 5 °C when pH increases from a low pH range (pH $\leqslant$9.0) to a high pH range (pH $\geqslant$10.0), reflecting kinetic effects associated with CO_2 diffusion through the membrane and CO_2 hydroxylation.
(5) A Δ_{47}-temperature equation can be obtained using average sample values for each temperature (excluding the two high pH samples at 5 °C):

$$\Delta_{47} = (0.0387 \pm 0.0072) \times 10^6/T^2 + (0.2532 \pm 0.0829)$$
$$(r^2 = 0.9998,\ p = 0.009)$$

This equation is useful to approximate equilibrium Δ_{47} precipitation and digestion at elevated temperatures for clumped isotope analysis.

(6)At current analytical precision, our Δ_{47}-temperature equation is apparently not sensitive to variation in pH, precipitation rate, and ionic strength (excluding the two high pH samples at 5 °C) and thus could represent a nominal equilibrium calibration line.

ACKNOWLEDGEMENTS

In this study, the part of inorganic calcite precipitation was funded by the European Scientific Foundation (ESF) project CASIOPEIA (DFG, Ei272/20-1/-2) and financially supported by the Austrian Science Fund (FWF I34-B06). J. Tang was supported by laboratory start-up funds granted to B.E. Rosenheim from the School of Science and Engineering of Tulane University, a considerable investment in technical staff that enabled the work performed in this manuscript. A. Tripati acknowledges support from Department of Energy BES grant DE-FG02-13ER16402, National Science Foundation grants from Instrumentation and Facilities, Low-Temperature Geochemistry, and Arctic Natural Sciences, ACS grant 51182-DNI2, a Hellman Fellowship, and a UCLA Career Development Award. We wish to thank the associate editor, Frank McDemott, the reviewer, Hagit P. Affek, and two

anonymous reviewers for their constructive comments and suggestions, which greatly improved this manuscript.

REFERENCES

Affek H. P. (2013) Clumped isotopic equilibrium and the rate of isotope exchange between CO_2 and water. *Am. J. Sci.* **313**, 309–325.

Affek H. P., Bar-Matthews M., Ayalon A., Mathews M. and Eiler J. M. (2008) Glacial/interglacial temperature variations in Sorequ cave speleothems as recorded by 'clumped isotope' thermometry. *Geochim. Cosmochim. Acta* **72**, 5351–5360.

Arienzo M., Swart P., Murray S. and Vonhof H. (2013) Temperature determination from speleothems through fluid inclusion and clumped isotope techniques. *Mineral. Mag.* **77**(5), 613.

Beck W. C., Grossman E. L. and Morse J. W. (2005) Experimental studies of oxygen isotope fractionation in the carbonic acid system at 15, 25 and 40 °C. *Geochim. Cosmochim. Acta* **69**, 3493–3503.

Came R. E., Eiler J. M., Veizer J., Azmy K., Brand U. and Weidman C. R. (2007) Coupling of surface temperatures and atmospheric CO_2 concentrations during the Palaeozoic era. *Nature* **449**, 198–201.

Cao X. and Liu Y. (2012) Theoretical estimation of the equilibrium distribution of clumped isotopes in nature. *Geochim. Cosmochim. Acta* **77**, 292–303.

Carpenter S. J. and Lohmann K. C. (1992) Sr/Mg ratios of modern marine calcite: empirical indicators of ocean chemistry and precipitation rate. *Geochim. Cosmochim. Acta* **56**, 1837–1849.

Coplen T. B. (2007) Calibration of the calcite–water oxygen-isotope geothermometer at Devils Hole, Nevada, a natural laboratory. *Geochim. Cosmochim. Acta* **71**, 3948–3957.

Daëron M., Guo W., Eiler J. M., Genty D., Blamart D., Boch R., Drysdale R., Maire R., Wainer K. and Zanchetta G. (2011) $^{13}C^{18}O$ clumping in speleothems: observations from natural caves and precipitation experiments. *Geochim. Cosmochim. Acta* **75**, 3303–3317.

Dennis K. J. and Schrag D. P. (2010) Clumped isotope thermometry of carbonatites as an indicator of diagenetic alteration. *Geochim. Cosmochim. Acta* **74**, 4110–4122.

Dennis K. J., Affek H. P., Passey B. H., Schrag D. P. and Eiler J. M. (2011) Defining the absolute reference frame for 'clumped' isotope studies of CO_2. *Geochim. Cosmochim. Acta* **75**, 7117–7131.

Dennis K. J., Cochran J. K., Landman N. H. and Schrag D. P. (2013) The climate of the Late Cretaceous: new insights from the application of the carbonate clumped isotope thermometer to Western Interior Seaway macrofossil. *Earth Planet. Sci. Lett.* **362**, 51–65.

DePaolo D. J. (2011) Surface kinetic model for isotopic and trace element fractionation during precipitation of calcite from aqueous solutions. *Geochim. Cosmochim. Acta* **75**(4), 1039–1056.

Dietzel M. and Usdowski E. (1996) Coprecipitation of Ni^{2+}, Co^{2+}, and Mn^{2+} with galena and covellite, and of Sr^{2+} with calcite during crystallization via diffusion of H_2S and CO_2 through polyethylene at 20 °C: power law and Nernst law control of trace element partitioning. *Chem. Geol.* **131**, 55–651.

Dietzel M., Gussone N. and Eisenhauer A. (2004) Co-precipitation of Sr^{2+} and Ba^{2+} with aragonite by membrane diffusion of CO_2 between 10 and 50 °C. *Chem. Geol.* **203**, 139–151.

Dietzel M., Tang J., Leis A. and Köhler S. J. (2009) Oxygen isotopic fractionation during inorganic calcite precipitation - Effects of temperature, precipitation rate and pH. *Chem. Geol.* **268**, 107–115.

Eagle R., Schauble E. A., Tripati A. K., Tütken T., Hulbert R. C. and Eiler J. M. (2010) Body temperatures of modern and extinct vertebrate from ^{13}C–^{18}O bond abundances in bioapatit. *PNAS* **107**, 10377–10382.

Eagle R., Tutken T., Martin T., Tripati A., Fricke H., Connely M., Cifelli R. and Eiler J. (2011) Dinosaur body temperatures determined from isotopic (^{13}C–^{18}O) ordering in fossil biominerals. *Science* **333**, 443–445.

Eagle R., Eiler J., Tripati A., Ries J., Freitas P., Hiebenthal C., Wanamaker, Jr., A., Taviani M., Elliot M., Marenssi S., Nakamura K., Ramirez P. and Roy K. (2013) The influence of temperature and seawater carbonate saturation state on ^{13}C–^{18}O bond ordering in bivalve mollusks. *Biogeosciences* **10**, 4591–4606.

Eiler J. M. (2007) "Clumped-isotope" geochemistry—the study of naturally-occurring multiply-substituted isotopologues. *Earth Planet. Sci. Lett.* **262**, 309–327.

Epstein S., Buchsbaum R., Lowenstam H. A. and Urey H. C. (1951) Carbonate-water isotopic temperature scale. *Geol. Soc. Am. Bull.* **62**, 417–426.

Epstein S., Buchsbaum R., Lowenstam H. A. and Urey H. C. (1953) Revised carbonate-water isotopic temperature scale. *Geol. Soc. Am. Bull.* **64**, 1315–1326.

Fernandez A., Tang J. and Rosenheim B. E. (2014) Siderite 'clumped' isotope thermometry: a new paleoclimate proxy for humid continental environments. *Geochim. Cosmochim. Acta* **116**, 411–421.

Flower B. P. and Kennett J. P. (1990) The Younger Dryas cool episode in the Gulf of Mexico. *Paleoceanography* **5**, 949–961.

Flower B. P., Hastings D. W., Hill H. W. and Quinn T. M. (2004) Phasing of deglacial warming and Laurentide ice sheet meltwater in the Gulf of Mexico. *Geology* **32**, 597–600.

Gaetani G. A., Cohen A. L., Wang Z. and Crusius J. (2011) Rayleigh-based, multi-element coral thermometry: a biomineralization approach to developing climate proxies. *Geochim. Cosmochim. Acta* **75**, 1920–1932.

Geisler T., Perdikouri C., Kasioptas A. and Dietzel M. (2012) Real-time monitoring of the overall exchange of oxygen isotopes between aqueous CO_3^{2-} and H_2O by Raman spectroscopy. *Geochim. Cosmochim. Acta* **90**, 1–11.

Ghosh P., Adkins J., Affek H., Balta B., Guo W., Schauble E. A., Schrag D. and Eiler J. M. (2006) ^{13}C–^{18}O bonds in carbonate minerals: a new kind of paleothermometer. *Geochim. Cosmochim. Acta* **70**, 1439–1456.

Ghosh P., Eiler J. M., Campana S. E. and Feeny R. F. (2007) Calibration of the carbonate 'clumped isotope' paleothermometer for otoliths. *Geochim. Cosmochim. Acta* **71**, 2736–2744.

Grauel A.-L., Schmid T. W., Hu B., Bergami C., Capotondi L., Zhou L. and Bernasconi S. M. (2013) Calibration and application of the 'clumped isotope' thermometer to foraminifera for high-resolution climate reconstructions. *Geochim. Cosmochim. Acta* **108**, 125–140.

Guo W. (2008) Carbonate clumped isotope thermometre: application to carbonaceaous chondrites and effects of kinetic isotope fractionation. Ph. D. thesis, California Institute of Technology.

Guo W., Mosenfelder J. L., Goddard, III, W. A. and Eiler J. M. (2009) Isotopic fractionations associated with phosphoric acid digestion of carbonate minerals: insights from first-principles theoretical modeling and clumped isotope measurements. *Geochim. Cosmochim. Acta* **73**, 7203–7225.

Gussone N., Böhm F., Eisenhauer A., Dietzel M., Heuser A., Teichert B. M. A., Reitner J., Wörheide G. and Dullo W.-C. (2005) Calcium isotope fractionation in calcite and aragonite. *Geochim. Cosmochim. Acta* **69**, 4485–4494.

He B., Olack G. A. and Colman A. S. (2012) Pressure baseline correction and high-precision CO2 clumped-isotope (Δ47)

measurements in bellows and micro-volume modes. *Rapid Commun. Mass Spectrom.* **26**, 2837–2853.

Hendy E. J., Gagan M. K., Alibert C. A., McCulloch M. T., Lough J. M. and Isdale P. J. (2002) Abrupt decrease in tropical Pacific Sea surface salinity at end of Little Ice Age. *Science* **295**, 1511–1514.

Henkes G. A., Passey B. H., Wanamaker, Jr., A. D., Grossman E. L., Ambrose, Jr., W. G. and Carroll M. L. (2013) Carbonate clumped isotope compositions of modern marine mollusk and brachiopod shells. *Geochim. Cosmochim. Acta* **106**, 307–325.

Hill P. S., Schauble E. A. and Tripati A. K. (2013) Theoretical constraints on the effects of pH, salinity, and temperature on clumped isotope signatures of dissolved inorganic carbon species and precipitating carbonate minerals. *Geochim. Cosmochim. Acta*. http://dx.doi.org/10.1016/j.gca.2013.06.018.

Huntington K. W., Eiler J. M., Affek H. P., Guo W., Bonifacie M., Yeung L. Y., Thiagarajan N., Passey B., Tripati A., Daëron M. and Came R. (2009) Methods and limitations of 'clumped' CO_2 isotope (Δ_{47}) analysis by gas-source isotope ratio mass spectrometry. *J. Mass Spectrom.* **44**, 1318–1329.

Kim S.-T. and O'Neil J. R. (1997) Equilibrium and nonequilibrium oxygen isotope effects in synthetic carbonates. *Geochim. Cosmochim. Acta* **61**, 3461–3475.

Kluge T. and Affek H. P. (2012) Quantifying kinetic fractionation in Bunker Cave speleothems using Δ_{47}. *Quatern. Sci. Rev.* **49**, 82–94.

Lund D. C. and Curry W. (2006) Florida Current surface temperature and salinity variability during the last millennium. *Paleoceanography* **21**, 15.

McConnaughey T. (1989) ^{13}C and ^{18}O isotopic disequilibrium in biological carbonates: II. *In vitro* simulation of kinetic isotope effects. *Geochim. Cosmochim. Acta* **53**, 163–171.

Moses C. S., Swart P. K. and Rosenheim B. E. (2006) Evidence of multi-decadal salinity variability in the eastern tropical North Atlantic. *Paleoceanography* **21**, PA3010, doi: 3010.1029/2005PA001257.

Passey B. H. and Henkes G. A. (2012) Carbonate clumped isotope bond reordering and geospeedometry. *Earth Planet. Sci. Lett.* **351–352**, 223–236.

Passey B. H., Levin N. E., Cerling T. E., Brown F. H. and Eiler J. M. (2010) High-temperature environments of human evolution in East Africa based on bond ordering in paleosol carbonates. *PNAS* **107**, 11245–11249.

Rosenheim B. E., Swart P. K., Thorrold S. R., Eisenhauer A. and Willenz P. (2005) Salinity change in the subtropical Atlantic: secular increase and teleconnections to the North Atlantic Oscillation. *Geophys. Res. Lett.* **32**.

Rosenheim B. E., Swart P. K. and Willenz Ph. (2009) Calibration of sclerosponge oxygen isotope records to temperature using high-resolution $\delta^{18}O$ data. *Geochim. Cosmochim. Acta* **73**, 11.

Rosenheim B. E., Tang J. and Fernandez A. (2013) Measurement of multiply-substituted isotopologues ("clumped isotopes") of CO_2 using a 5kV compact isotope ratio mass spectrometer: performance, reference frame, and carbonate paleothermometry. *Rapid Commun. Mass Spectrom.* **27**, 1847–1857.

Saenger C., Affek H. P., Felis T., Thiagarajan N., Lough J. M. and Holcomb M. (2012) Carbonate clumped isotope variability in shallow water corals: temperature dependence and growth-related vital effects. *Geochim. Cosmochim. Acta* **99**, 224–242.

Schauble E. A., Ghosh P. and Eiler J. M. (2006) Preferential formation of ^{13}C–^{18}O bonds in carbonate minerals, estimated using first-principles lattice dynamics. *Geochim. Cosmochim. Acta* **70**, 2510–2529.

Schmidt G. A. (1999) Error analysis of paleosalinity calculations. *Paleoceanography* **14**, 422–429.

Schmidt M. W. and Lynch-Stieglitz J. (2011) Florida Straits deglacial temperature and salinity change: implications for tropical hydrologic cycle variability during the Younger Dryas. *Paleoceanography* **26**.

Schmidt M. W., Spero H. J. and Lea D. W. (2004) Links between salinity variation in the Caribbean and North Atlantic thermohaline circulation. *Nature* **428**, 160–163.

Schmidt M. W., Vautravers M. J. and Spero H. J. (2006) Rapid subtropical North Atlantic salinity oscillations across Dansgaard–Oeschger cycles. *Nature* **443**, 561–564.

Spero H. J. and Williams D. F. (1990) Evidence for seasonal low-salinity surface waters in the Gulf of Mexico over the last 16,000 years. *Paleoceanography* **5**, 963–975.

Tang J., Köhler S. J. and Dietzel M. (2008) Sr^{2+}/Ca^{2+} and $^{44}Ca/^{40}Ca$ fractionation during inorganic calcite formation: I. Sr incorporation. *Geochim. Cosmochim. Acta* **72**, 3718–3732.

Tang J., Niedermayr A., Köhler S. J., Böhm F., Kısakürek B., Eisenhauer A. and Dietzel M. (2012) Sr^{2+}/Ca^{2+} and $^{44}Ca/^{40}Ca$ fractionation during inorganic calcite formation: III. Impact of salinity/ionic strength. *Geochim. Cosmochim. Acta* **77**, 432–443.

Thiagarajan N., Adkins J. and Eiler J. (2011) Carbonate clumped isotope thermometry of deep-sea corals and implications for vital effects. *Geochim. Cosmochim. Acta* **75**, 4416–4425.

Tripati A. K., Eagle R. A., Thiagarajan N., Gagnon A. C., Bauch H., Halloran P. R. and Eiler J. M. (2010) ^{13}C–^{18}O isotope signatures and 'clumped isotope' thermometry in foraminifera and coccoliths. *Geochim. Cosmochim. Acta* **74**, 5697–5717.

Tripati A. K., Hill P., Eagle R., Schauble E., Eiler J., Zeebe R. and Uchikawa J. (in revision) ^{13}C–^{18}O bond ordering and $^{18}O/^{16}O$ ratios in dissolved inorganic carbon species and their potential to be preserved in the solid phase. *Earth Planet. Sci. Lett*.

Urey H. C. (1947) The thermodynamic properties of isotopic substances, Chemical Society in the Royal Institution. *J. Chem. Soc.* **1947**, 562–581.

Usdowski E., Michaelis J., Böttcher M. E. and Hoefs J. (1991) Factors for the oxygen isotope equilibrium fractionation between aqueous and gaseous CO2, carbonic acid, bicarbonate, carbonate, and water (19 °C). *Z. Phys. Chem.* **170**, 237–249.

Wang Z., Schauble E. A. and Eiler J. M. (2004) Equilibrium thermodynamics of multiply substituted isotopologues of molecular gases. *Geochim. Cosmochim. Acta* **68**, 4779–4797.

Watson E. B. (2004) A conceptual model for near-surface kinetic controls on the trace-element and stable isotope composition of abiogenic calcite crystals. *Geochim. Cosmochim. Acta* **68**, 1473–1488.

Zaarur S., Olack G. and Affek H. P. (2011) Paleo-environmental implication of clumped isotopes in land snail shells. *Geochim. Cosmochim. Acta* **75**, 6859–6869.

Zaarur S., Affer H. P. and Brandon M. T. (2013) A revised calibration of the clumped isotope thermometer. *Earth Planet. Sci. Lett.* **382**, 47–57.

Zeebe R. E. (1999) An explanation of the effect of seawater carbonate concentration on foraminiferal oxygen isotopes. *Geochim. Cosmochim. Acta* **63**, 2001–2007.

Associate editor: F. McDermott